28. T. Holstein, *Ann. Phys.* **8**, 343 (1959).
29. D. Emin, T. Holstein, *Phys. Rev. Lett.* **36**, 323 (1976).
30. V. V. Kabanov, O. Y. Mashtakov, *Phys. Rev. B* **47**, 6060 (1993).
31. H. Sumi, A. Sumi, *J. Phys. Soc. Jpn.* **63**, 637 (1994).
32. G. Kalosakas, S. Aubry, G. P. Tsironis, *Phys. Rev. B* **58**, 3094 (1998).

33. We thank C. Wittig for valuable discussions. Supported by the director, Office of Energy Research, Office of Basic Energy Sciences, Chemical Sciences Division of the U.S. Department of Energy, under contract DE-AC03-76SF00098. We acknowledge NSF support for specialized equipment used in these experiments.

Supporting Online Material
www.sciencemag.org/cgi/content/full/297/5584/1163/DC1
SOM Text
References and Notes

3 May 2002; accepted 10 July 2002

Rotationally Resolved Infrared Spectrum of the Charge Transfer Complex $[Ar–N_2]^+$

H. Linnartz,* D. Verdes, J. P. Maier

Difficulties in preparing cluster ions for spectroscopic studies have limited our understanding of intermolecular forces in charged complexes that are typical of many reactive intermediates. Here, the infrared spectrum of the charge transfer complex $[Ar–N_2]^+$, recorded in a supersonic planar plasma with a tunable diode laser spectrometer, is presented. More than 70 adjacent rovibrational transitions were measured near 2272 wave numbers and assigned to the molecular nitrogen stretching fundamental in the $^2\Sigma^+$ ground state of $[Ar–N_2]^+$. The accurate structural parameters that were determined confirm a linear structure and show that the major part of the charge is located at the argon atom. The latter result is surprising and implies a charge switch of the cationic center upon complexation.

A good understanding of intermolecular forces, such as van der Waals interactions or hydrogen bonds, is essential for the description of the chemical and physical properties of matter (*1*). However, although weakly bound neutral complexes have been studied extensively in the past, high-resolution information about polyatomic ionic complexes is limited (*2*). These complexes have binding energies that are typically between those of pure van der Waals and covalent bonds and play a key role as reactive intermediates in many processes. An accurate spectroscopic characterization, therefore, is necessary to understand the structural and dynamical characteristics of cluster ions at the fundamental level of molecular motion.

This is particularly true for the charge transfer complex $[Ar–N_2]^+$, which has been puzzling researchers for two decades. Upon photodissociation, the complex fragments mainly via the decay channel $Ar^+ (^2P_{3/2}) + N_2(X^1\Sigma)$, but the $N_2^+ (X^2\Sigma) + Ar (^1S)$ channel should be energetically preferred (*3*). A similar anomaly is observed in experiments studying the charge transfer process $Ar^+(^2P_{3/2}) + N_2(X^1\Sigma_{v=0}) \rightarrow Ar + N_2^+(X^2\Sigma_{v=v'})$ (*4*). Although the reaction is exothermic by nearly 0.18 eV, its reactivity is typical of that for an endothermic process. These findings indicate that $[Ar–N_2]^+$ is formed in the recombination of Ar with N_2^+ rather than Ar^+ with N_2, but upon photodissociation, the complex fragments into $Ar^+ + N_2$ rather than $Ar + N_2^+$. This special dynamical behavior has been explained in terms of a curve crossing between the states correlating to $N_2^+(X^2\Sigma)/Ar(^1S)$ and $Ar^+(^2P_{3/2})/N_2(X^1\Sigma)$ (*3*). The potential energy surface (PES) of the latter (higher lying) state diabatically correlates to the strongly bound ground state of $[Ar–N_2]^+$, whereas the other (lower lying) state correlates to a repulsive state that is accessed from the ground state by the photon that induces the dissociation [see figure 10 of (*3*)]. Detailed information is now available for the photodissociation and charge transfer dynamics of the $[Ar–N_2]^+$ species, providing state-to-state cross sections, reaction rates, rotational and vibrational energy distributions of the products, and details of the low-lying PES (*3–9*). However, a high-resolution study of the ground state of the reactive intermediate $[Ar–N_2]^+$ has been lacking up to now.

This lack of information is mainly due to the difficulties involved in producing a large abundance of cluster ions under laboratory conditions. Recent progress in the generation of dense supersonic planar plasma expansions has made a more general detection scheme of ionic complexes with direct absorption spectroscopy possible (*10*, *11*). Such a plasma offers a nearly Doppler-free environment and combines high molecular densities and a low final temperature (<20 K) with a relatively long absorption path length. The experimental method applied here is based on the absorption of tunable infrared radiation in a planar plasma that is generated by electron impact ionization with the use of a supersonic ion jet diode laser spectrometer (*12*, *13*).

We report the detection and analysis of the rovibrational spectrum of $[Ar–N_2]^+$ in its $^2\Sigma$ ground state. More than 70 adjacent vibration-rotation lines have been observed around 2272 cm^{-1}, with an intensity distribution that corresponds to a rotational temperature of about 15 K (*13*). The spectrum is that of a $^2\Sigma–^2\Sigma$ transition of a linear molecule and consists of a progression of P- and R-branch doublets, apart from very low rotational quantum numbers where the Q-branch transitions are still intense enough to be detectable. Parts of the spectrum are shown in Fig. 1.

The assignment of these transitions to the molecular nitrogen (NN) stretching vibration of linear $[Ar–N_2]^+$ is straightforward, even though the experiment was not mass selective and other species were produced in the plasma as well. The signal was not observed without Ar or N_2 in the expansion, which excluded pure Ar or N_2 clusters, and scaled linearly with the $[Ar–N_2]^+$ mass signal. The latter signal was strong, as may be expected; the ionization potentials (IPs) of Ar (15.760 eV) and N_2 (15.581 eV) are almost identical (*15*), tending to form a bond with a covalent character upon complexation. Kinetic energy release studies have found a binding energy for $[Ar–N_2]^+$ as high as 1.19 eV, which is comparable, for example, to the value found for the homonuclear species Ar_2^+ (1.29 eV)

Table 1. Molecular parameters describing the rotational (B_v), distortion (D_v), and spin-rotation (γ_v) constants of $[Ar–N_2]^+$ in its electronic $^2\Sigma$ ground state for $v = 0$ and upon vibrational excitation of the NN fundamental ($v = 1$). All values are given in wave numbers. The numbers in parentheses indicate 1σ deviations.

	ν_{01}	B_v	D_v ($\times 10^{-8}$)	γ_v
$v = 0$	0	0.128712(10)	8.9(26)	−0.01065(16)
$v = 1$	2272.2564(2)	0.128212(10)	9.4(22)	−0.01056(16)

Department of Chemistry, Klingelbergstrasse 80, CH-4056 Basel, Switzerland.

*To whom correspondence should be addressed. E-mail: Henricus.Linnartz@unibas.ch

(*16*). Further evidence is provided by analyzing the rotational spectrum. The electronic ground state of $[Ar–N_2]^+$ has $^2\Sigma^+$ character that is due to a mixing of the $3\sigma_g$ molecular orbital of N_2^+ with the 3p(Ar) atomic orbital. This forms an intermolecular pair of levels with two electrons in the bonding level and one in the antibonding level. All observed transitions were described within a fit routine (*17*) using a standard Hamiltonian for a linear molecule in a $^2\Sigma$ state, with terms representing the rotational (B_v), centrifugal distortion (D_v), and spin-rotation interaction (γ_v) constants in ground ($v = 0$) and vibrationally excited ($v = 1$) state. This procedure gives an excellent fit (see Fig. 1 for details) with a standard deviation of less than 0.0007 cm^{-1}. The resulting molecular parameters are listed in Table 1.

The rotational constant B can be directly compared to ab initio calculations (*18–21*). These calculations predict a linear equilibrium geometry for $[Ar–N_2]^+$ with an intramolecular distance r(NN) on the order of 1.1 Å and an intermolecular distance r(Ar-N) around 2.2 Å. Theses values give a rotational constant for the equilibrium structure $B_e \sim 0.127$ cm^{-1}, close to the experimental value found here: $B_0 \sim 0.1287$ cm^{-1}. It was concluded in these studies that the calculated value for r(NN) is shorter than the intermolecular bond length of free N_2^+ and almost identical to that of a neutral N_2 molecule. This result implies a charge switch of the cationic center from the molecule with the lower IP (N_2) to the atom with the higher IP (Ar). The vibrational analysis of the spectrum observed here confirms the occurrence of a charge switch. The position of the band origin can be related in a first approximation to the amount of N_2^+ (fundamental at 2175 cm^{-1}) or N_2 (fundamental at 2330 cm^{-1}) character the excited vibration has, and this approach has been used previously to conclude that the charge is strongly delocalized in $[N_2–N_2]^+$, partly delocalized in $N_2–Ar^{(+)}–N_2$, and completely localized in $N_2–H^+–N_2$ (*22–24*). The band origin of the $v = 0 \rightarrow 1$ vibrational excitation of $[Ar–N_2]^+$ is found at 2272 cm^{-1}, closer to the N_2 fundamental, indicating that the major part of the charge is located at the Ar atom. In a series of ab initio calculations, this amount is predicted to be between 65 and 85% (*19–21*).

There has been much interest in the cluster ions generated in Ar and N_2 plasmas. The high-resolution infrared data presented here provide a fingerprint spectrum to search for $[Ar–N_2]^+$ in such environments. They show that the complex has a linear ground state geometry and that a shift of the cationic center is induced upon complexation. The present study provides constants that are accurate enough to guide a spectroscopic search for $[Ar–N_2]^+$ in the microwave range. Such a study is capable of resolving splittings due to hyperfine interactions, and it is likely that this will provide additional information on the charge distribution in the $[Ar–N_2]^+$ complex.

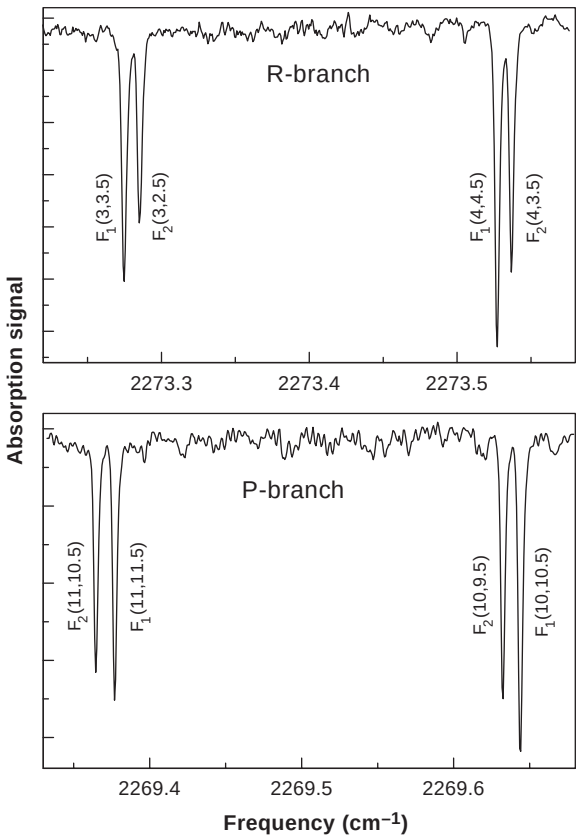

Fig. 1. Parts of the P (**bottom**) and R (**top**) branch of the rovibrational spectrum in the electronic ground state of $[Ar–N_2]^+$ upon vibrational excitation of the NN stretch. The rotational progression in a $^2\Sigma$ state is given by $F_1(N,J) = B_vN(N + 1) – D_vN^2(N + 1)^2 + 0.5\ \gamma_vN$ for a total angular momentum $J = N + 1/2$ and by $F_2(N,J) = B_vN(N + 1) – D_vN^2(N + 1)^2 – 0.5\ \gamma_v\ (N + 1)$ for $J = N – 1/2$, where N represents the rotational quantum number. Upon vibrational excitation, these values shift by ν_{01}, the value for the position of the band origin. Transitions with $\Delta J = 0$ and ± 1 are allowed. The intensity of transitions with $\Delta J = 0$ falls off rapidly with increasing N. As a consequence, Q-branch transitions are only observed for very low N values, and the major part of the spectrum is dominated by a doublet structure because of spin-rotation interaction (*14*), as can be seen in the figure. More than 30 doublets were observed in the range from 2267.7 to 2277.0 cm^{-1}. A fit gives accurate values for the band origin and for the constants B_v, D_v, and γ_v in the ($v = 0$) and vibrationally excited ($v = 1$) state (Table 1). In the absence of Q-branch transitions that connect levels with different symmetry [that is, $F_1(N,J)$ and $F_2(N,J)$], it is difficult to distinguish between P_1 and P_2 (or R_1 and R_2) branches and thus it is hard to determine the sign of γ_v. However, in the case of high-quality spectra, the sign can also be determined on the basis of intensity considerations. Because the line strength of the P_1 and R_1 transitions is greater than that of the corresponding P_2 and R_2 transitions by a factor $[(N + 1)/(N)]$, we can unambiguously assign a negative value for γ (Table 1).

References and Notes

1. P. E. S. Wormer, A. van der Avoird, *Chem. Rev.* **100**, 4109 (2000).
2. E. J. Bieske, O. Dopfer, *Chem. Rev.* **100**, 3963 (2000).
3. H. S. Kim, M. T. Bowers, *J. Chem. Phys.* **93**, 1158 (1990).
4. R. Candori *et al.*, *J. Chem. Phys.* **115**, 8888 (2001) and references therein.
5. D. M. Sonnenfroh, S. R. Leone, *J. Chem. Phys.* **90**, 1677 (1989).
6. D. C. Clary, D. M. Sonnenfroh, *J. Chem. Phys.* **90**, 1686 (1989).
7. R. H. Schultz, P. B. Armentrout, *Chem. Phys. Lett.* **179**, 429 (1991).
8. T. F. Magnera, J. Michl, *Chem. Phys. Lett.* **192**, 99 (1992).
9. A. A. Viggiano, R. A. Morris, *J. Chem. Phys.* **99**, 3527 (1993).
10. S. Davis, D. T. Anderson, G. Duxbury, D. J. Nesbitt, *J. Chem. Phys.* **107**, 5661 (1997).
11. T. Motylewski, H. Linnartz, *Rev. Sci. Instrum.* **70**, 1305 (1999).
12. H. Linnartz, D. Verdes, T. Speck, *Rev. Sci. Instrum.* **71**, 1811 (2000).
13. A schematic drawing, a short description of the experimental setup, and a list with line positions and observed-calculated values are available as supplementary material on *Science* Online.
14. G. Herzberg, *Molecular Spectra and Molecular Structure I* (Krieger Publishing, Malabar, FL, reprint ed., 1989).
15. G. Lias *et al.*, *J. Phys. Chem. Ref. Data* **17** (suppl. 1), 1 (1988).
16. K. M. Weitzel, J. Mähnert, *Int. J. Mass Spectrom. Ion Processes* **214**, 175 (2002).
17. PGOPHER, 1994 and 1998; C. M. Western, School of Chemistry, University of Bristol, UK.
18. V. Frecer, D. C. Jain, A.-M. Sapse, *J. Phys. Chem.* **95**, 9263 (1991).
19. K. Hiraoka, T. Mori, S. Yamabe, *Chem. Phys. Lett.* **189**, 7 (1992).
20. J. Mähnert, H. Baumgärtel, K. M. Weitzel, *J. Chem. Phys.* **102**, 180 (1995).
21. J. H. Langenberg, I. B. Bucur, P. Archirel, *Chem. Phys.* **221**, 225 (1997).
22. T. Ruchti *et al.*, *J. Chem. Phys.* **105**, 2591 (1996).
23. D. Verdes *et al.*, *J. Chem. Phys.* **111**, 8400 (1999).
24. H. Linnartz *et al.*, *J. Chem. Phys.* **113**, 895 (2000).

25. Supported by the Swiss National Science Foundation, project 20.63459.00. We are thankful for helpful discussions with P. J. Knowles, Birmingham. H.L. acknowledges support from the Fundamenteel Onderzoek der Materie.

Supporting Online Material

www.sciencemag.org/cgi/content/full/297/5584/1166/DC1
Materials and Methods
Fig. S1
Table S1
References and Notes

21 May 2002; accepted 8 July 2002